CHEMPHYSCHEM

DOI: 10.1002/cphc.200800080

CO Adsorption on a $LaNi_5$ Hydrogen Storage Alloy Surface: A Theoretical Investigation

Song Han,[a] Xin-Bo Zhang,[a] Si-Qi Shi,[a, c] Masanori Kohyama,[a] Hideaki Tanaka,[a] Nobuhiro Kuriyama,[a] Naoki Taoka,[b] Teruo Kaneko,[b] and Qiang Xu*[a]

Density functional theory calculations are carried out to study CO adsorption on the (001) surface of a $LaNi_5$ hydrogen storage alloy. At low coverages, CO favors adsorption on Ni–Ni bridge sites. With an increase in CO coverage, the decrease in the adsorption energy is much larger for Ni–Ni–CO bridge adsorption than that for Ni–CO on-top adsorption. Thus, the latter sites in the relatively stable adsorption structure are preferentially utilized at high CO coverages. The nature of the bonding between CO and the $LaNi_5$ (001) surface is analyzed in detail.

1. Introduction

With greenhouse gas emissions affecting political and environmental climates, the need for alternative fuels has become abundantly clear.[1,2] Hydrogen, as an ideal energy carrier, is of great interest to meet the challenges of environmental pollution and the pending energy crisis.[3] On the way to a hydrogen-energy society, a safe, effective, and low-cost hydrogen-storage system is crucial.[4] Among different hydrogen storage systems, hydrogen storage alloys are important and have been widely used.[5,6] Extensive experimental work has been done on their structures and properties, and theoretical calculations based on DFT have made important contributions to the understanding of their structures and stabilities.[7–9] For practical applications, hydrogen storage alloys must resist deterioration due to unavoidable impurities, such as carbon monoxide, present in hydrogen produced by steam reforming.[10]

Work on the hydrogen absorbing–desorbing cycle durability by using H_2 with 300 ppm O_2, H_2O or CO has revealed that the presence of CO has the severest effect on hydrogen storage ability.[11] Systematic investigations on the cyclic durability of Ca–Mg–Ni and Ti–V alloys with pure H_2 and with CO-contaminated H_2 indicate that the hydrogen storage capacities of the alloys decrease seriously with increasing CO concentration. Surprisingly, though, the crystal structures of bulk alloys before and after absorbing–desorbing cycles remain almost unchanged.[12,13] Is the devitalization of alloy surfaces responsible for the deterioration of their hydrogen storage ability? It is important to shed light on the degradation mechanism of the alloys.

Although there have been a number of reports on CO adsorption on pure metal surfaces,[14–18] less is known about CO adsorption on alloy surfaces.[19–21] Herein, we investigate CO adsorption on the surface of a $LaNi_5$ hydrogen storage alloy with DFT.

Computational Methods

First-principle calculations were performed within the framework of DFT using a basis set consisting of plane waves, as implemented in the Vienna ab initio simulation package (VASP).[22–24] The electron–ion interactions were described by projector-augmented wave (PAW)[25,26] pseudopotentials and the electron exchange and correlation energies were calculated with the Perdew and Wang (PW91)[27] formulation of the generalized gradient approximation.

A five-layer slab, separated by a vacuum layer of 14 Å, was used to model the $LaNi_5$ (001) surface. In order to ensure accuracy, all the atom layers were fully relaxed. Brillouin zone sampling was done on Monkhorst–Pack special points.[28] The plane-wave energy cutoff was set to 700 and 800 eV for geometry optimizations and static energy calculations, respectively. The *k*-point mesh was (6×6×6), (6×6×1) and (2×2×1) in the bulk $LaNi_5$, $p(1\times1)$ and $p(2\times2)$ cells, respectively. The Fermi level was smeared with a width of 0.2 eV by the Gaussian method.[29] This set of parameters assures a total energy convergence of 0.002 eV per atom. In the structural search, all the atoms were relaxed simultaneously. The search was stopped when forces on all atoms were less than 0.02 eV $Å^{-1}$. The convergence of the total energy with respect to the *k*-point meshes was also tested by increasing the *k*-point meshes from (6×6×6) to (8×8×8) for bulk $LaNi_5$. The change in total energy was only 0.002 eV, which is negligible, and no changes in structural parameters were found. The CO coverage (θ) is defined as the number of adsorbed CO molecules over the number of the atoms of the first layer. For

[a] *Dr. S. Han, Dr. X.-B. Zhang, Dr. S.-Q. Shi, Dr. M. Kohyama, Dr. H. Tanaka, Dr. N. Kuriyama, Prof. Q. Xu*
National Institute of Advanced Industrial Science and Technology (AIST)
Ikeda, Osaka 563-8577 (Japan)
Fax: (+81)72-751-9629
E-mail: q.xu@aist.go.jp

[b] *Dr. N. Taoka, Dr. T. Kaneko*
New Material Center (NMC), Osaka Science and Technology Center (OSTEC)
Nishi-Ku, Osaka 550-0004 (Japan)

[c] *Dr. S.-Q. Shi*
Department of Physics
Center for Optoelectronics Materials and Devices
Zhejiang Sci-Tech University, Xiasha College Park, Hangzhou 310018 (China)

Supporting information for this article is available on the WWW under http://dx.doi.org/10.1002/cphc.200800080.

example, one CO molecule on a $p(1\times1)$ surface corresponds to a coverage of 1/3 of a monolayer (ML) and one CO on $p(2\times2)$ to a coverage of 1/12 ML. The adsorption energy[30] per CO molecule is defined as $E_{ads}=\{E(\text{slab}/n\text{CO})-[E(\text{slab})+E(n\text{CO})]\}/n$, where E(slab/nCO) is the energy of the surface with adsorbed CO molecules, E(slab) that of the bare surface, $E(n\text{CO})$ that of gas phase CO and n the number of adsorbed CO molecules. Thus, the more negative the energy, the stronger the adsorption. Our calculations yield $LaNi_5$ lattice constants of 5.022 Å (a) and 3.978 Å (c), which agree with the experimental values of 5.017 Å (a) and 3.982 Å (c).[5] The calculated C–O bond length of gas phase is 1.144 Å, which is very close to the experimental length of 1.128 Å.[31]

2. Results and Discussion

2.1. Clean $LaNi_5$ (001) Surface

It is well-known that $LaNi_5$ alloys pulverize along the (001) surface during absorption/desorption cycles. Thus, for the theoretical calculations, we assume that the (001) surface is the mode surface. As shown in Figure 1, the $LaNi_5$(001) surface is an ideal

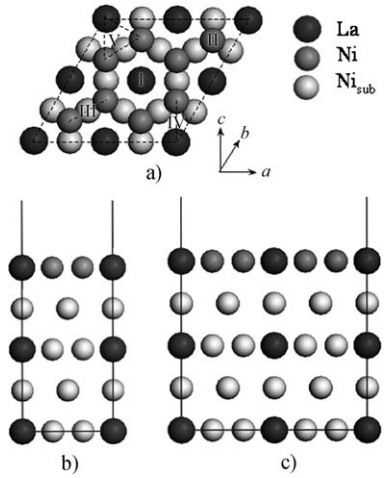

Figure 1. Top and side views of the $LaNi_5$(001) surface. a) Two on-top (I and II), two bridge (III and IV) and one hollow (V) sites for CO adsorption on the $p(2\times2)$ surface; b) side view of the $p(1\times1)$ slab; c) side view of the $p(2\times2)$ slab.

flat surface with 12 atoms (4 La and 8 Ni atoms) per $p(2\times2)$ unit cell. The relaxation of our five-layer slab is tabulated in Table 1, where d_{ik} denotes spacing between the i_{th} and k_{th} atom layer, and d_0 the bulk $LaNi_5$ spacing. The results show that the first and second layers shift outward and inward, respectively. Moreover, changes in the topmost interlayer spacing and the second interlayer spacing are all much lower than 4.0% and 1.0%, respectively, indicating that the bulk feature is recovered in the second layer. This indicates that the present slab thickness seems to be enough.

Table 1. Relaxation of the $LaNi_5$ (001) surface. d_{ik} is spacing between the i_{th} and k_{th} atom layers.

d_{ik}	Spacing after relaxation [Å]	Relaxation percentage [%][a]
d_{21}	2.0570	+3.4%
d_{32}	1.9809	−0.4%
d_{43}	1.9809	−0.4%

[a] Calculated as $(d_0-d_k)/d_0$; d_0 denotes the bulk $LaNi_5$ spacing of 1.9893 Å.

2.2. CO Adsorption States on the $LaNi_5$(001) Surface

The first-principle calculation method is employed to clarify the adsorption states of CO on the $LaNi_5$(001) surface. To fully investigate the CO adsorption on the surface at any coverage, end-on adsorptions are considered for all the possible sites, namely two on-top sites (I, II), two bridge sites (III, IV) and one hollow site (V), as indicated in Figure 1. Side-on adsorptions are considered for the bridge and hollow sites. Interestingly, after full relaxation, all the side-on adsorption configurations are energetically unstable at any coverage. Thus, we only discuss the relatively stable end-on adsorption configurations shown in Figure 2.

2.2.1. Low CO Coverages ($\theta=1/12$ and 1/6 ML)

The CO adsorption on the $LaNi_5$(001) surface is studied at low coverages of 1/12 and 1/6 ML. Three energetically stable adsorption sites are found for each case, namely the on-top and

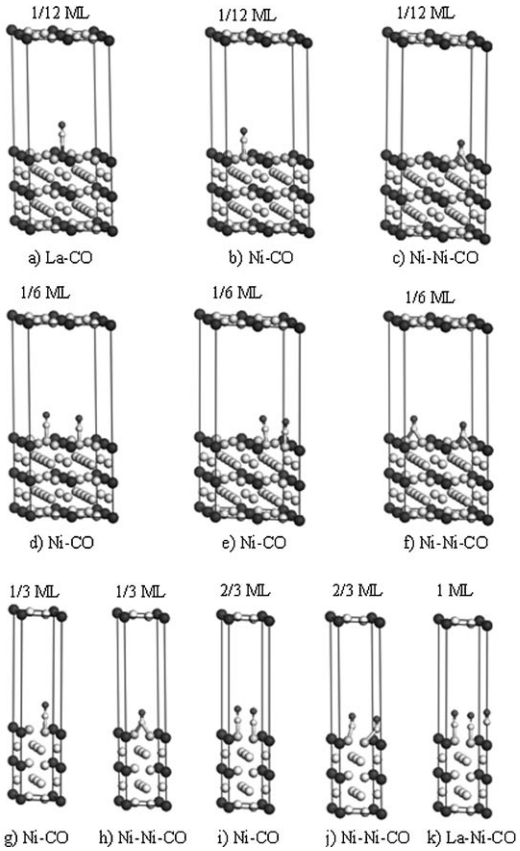

Figure 2. Schematic views of the configurations of CO adsorption on the (001) surface of the $LaNi_5$ hydrogen storage alloy.

Table 2. Structural and energetic properties of CO adsorbed on the $p(2\times2)$ $LaNi_5$(001) surface.

Configuration[a]	θ [ML]	Site	E_{ads} [eV]	d_{C-O} [Å]	d_{C-M} [Å]	d_{O-M} [Å]
a	1/12	La–CO on-top	0.462	1.149	2.760	–
b	1/12	Ni–CO on-top	2.066	1.179	1.734	–
c	1/12	Ni–Ni–CO bridge	2.180	1.205	1.885	1.885
d	1/6	Ni–CO on-top–1	1.991	1.177	1.736	–
e	1/6	Ni–CO on-top–2	1.989	1.177	1.734	–
f	1/6	Ni–Ni–CO bridge	1.933	1.203	1.910	1.910
g	1/3	Ni–CO on-top	1.984	1.175	1.735	–
h	1/3	Ni–Ni–CO bridge	1.931	1.196	1.905	1.905
i	2/3	Ni–CO on-top	1.815	1.168	1.746	–
j	2/3	Ni–Ni–CO bridge	1.499	1.183	1.923	1.923
k	1	La–CO/Ni–CO	1.258	1.137(La)	3.148	–
				1.173(Ni)	1.735	–

[a] Corresponding to sequence numbering in Figure 2.

bridge sites shown in Figures 2 a–f. Their bond parameters and adsorption energies are given in Table 2.

Configuration a) corresponds to CO on-top adsorption on the La atom. The C–O distance is 1.149 Å, which is very close to that of gas phase CO (1.128 Å). Moreover, based on its low adsorption energy (0.462 eV) and the long distance between C and La (2.760 Å), we can reasonably conclude that CO is weakly adsorbed on the La atom.

In the case of configuration b), CO is adsorbed on the Ni on-top site. The C–O and C–Ni distances are 1.179 and 1.734 Å, respectively, which are very similar to those on pure Ni surfaces.[18,32] The adsorption energy is 2.066 eV, which is much higher than that of configuration a).

In configuration c), CO is adsorbed on the bridge site of two Ni atoms. The C–O distance is 1.205 Å, which is longer than those of the La on-top (1.149 Å) and Ni on-top (1.179 Å) adsorptions. Its adsorption energy is 2.180 eV, which is the highest among the three cases. Thus, at low coverage, CO preferentially adsorbs on the bridge site of the two Ni atoms. This observation is consistent with previously obtained experimental and theoretical results for CO adsorption on pure Ni surfaces.[18]

At a coverage of 1/6 ML, after full relaxation, we finally obtain three stable adsorption configurations (d–f). Among them, two are Ni on-top adsorptions (d and e) and the other is a Ni–Ni bridge-site adsorption (f). The bond parameters and adsorption energies of d) and e) are very close to each other, as listed in Table 2. Interestingly, upon increasing the CO coverage from 1/12 to 1/6 ML, the adsorption energies decrease from 2.066 (on-top) and 2.180 eV (bridge) to 1.991 (on-top) and 1.933 eV (bridge), accompanied by a decease in the C–O distances from 1.179 (on-top) and 1.205 Å (bridge) to 1.177 (on-top) and 1.203 Å (bridge), respectively.

2.2.2. High CO Coverages ($\theta = 1/3$, 2/3, and 1 ML)

At a CO coverage of 1/3 ML, we obtain only two stable configurations (g and h), as shown in Figure 2 and Table 2. Upon increasing the CO coverage from 1/6 to 1/3 ML, the adsorption energies decrease from 1.991 (on-top) and 1.933 eV (bridge) to 1.984 (on-top) and 1.931 eV (bridge). The C–O distances also decrease, from 1.177 Å (on-top) and 1.203 Å (bridge) to 1.175 (on-top) and 1.196 Å (bridge), suggesting that the adsorption strengths of CO decrease with an increase in CO coverage. This trend is further confirmed by the adsorption energies and C–O distances at a CO coverage of 2/3 ML (i and j). The adsorption energy at the Ni–Ni bridge site (1.499 eV) is much lower than that at the Ni on-top site (1.815 eV), indicating that CO is ready to be adsorbed at the Ni on-top sites at a coverage of 2/3 ML.

At a coverage of 1 ML, the CO molecules are adsorbed on on-top sites of all the La and Ni atoms. The distance between the C and La atoms is 3.148 Å, which is very close to the sum of their van der Waals radii (C: 1.7 Å and La: 1.95 Å). Moreover, the C–O distance at the La site is 1.137 Å, which is close to that of gas phase CO. It is suggested that the CO adsorption is very weak at the La site, and that CO adsorption at 1 ML is not stable.

The CO coverage dependence of the adsorption energies of CO on the Ni sites of the (001) surface of the $LaNi_5$ hydrogen storage alloy is given in Figure 3. With an increase in CO coverage, the CO adsorption strength decreases. Most importantly, the Ni–Ni–CO bridge adsorptions are more stable than the on-top adsorptions at low CO coverages. On the other hand, at high CO coverages the on-top adsorptions become more stable than the Ni–Ni–CO bridge adsorptions.

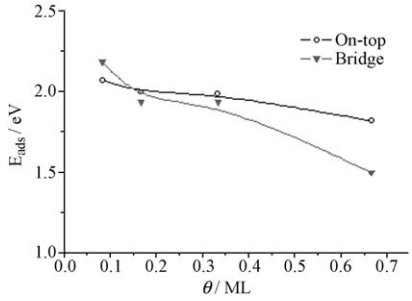

Figure 3. CO coverage dependence of the adsorption energies of CO on the Ni sites of (001) surface of the $LaNi_5$ hydrogen storage alloy.

2.3. Electronic Structure and Density of States

In order to investigate the nature of the bonding between CO and the $LaNi_5$(001) surface, the partial density of states (PDOS) for the three adsorption configurations (a, b and c) of the adsorbed CO and the surface metal atoms directly beneath the CO is analyzed at a coverage of 1/12 ML (Figures 4, 6 and 8).

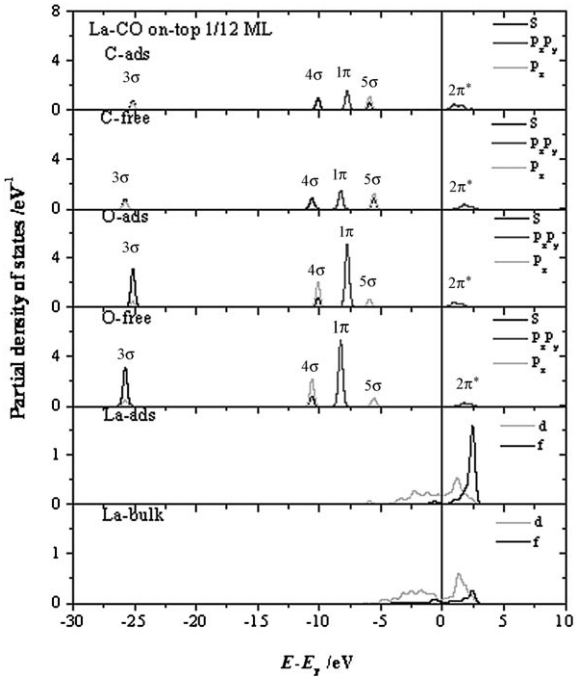

Figure 4. The PDOSs of CO on-top adsorption on a La atom of the $LaNi_5$ (001) surface ($\theta = 1/12$ ML). E_F is referenced as zero.

The PDOS for free CO [a CO molecule located at 7 Å above the $LaNi_5$(001) surface] and the clean surface metal atoms have also been calculated for comparison. The Fermi level lies at 0 eV and is marked by a solid vertical line. For free CO, the peaks from left to right represent the occupied 3σ (−25.8 eV), 4σ (−10.6 eV), 1π (−8.3 eV), 5σ (−5.6 eV), and unoccupied 2π (+1.8 eV) derived states, respectively, which are consistent with reported results.[33] The absence of PDOS peaks of the $LaNi_5$ side in the energy range around the 3σ level indicates that the 3σ molecular orbital is not involved in bonding with the $LaNi_5$ surface in any case. Thus, the upward shifts of the 3σ level upon progressing from free CO to the adsorption systems may be caused by the variation in the CO bond length and/or the electrostatic potential shift due to the charge transfer or dipole at the CO/substrate interface. The effect of the bond length is confirmed by static energy calculations of orbital shifts of a single CO molecule with the same bond length change as each adsorption system (Table 3). The longer the bond stretching, the larger the upward shift of the 3σ orbital of CO. However, it is clear that the full extent of the shifts cannot be explained solely by bond stretching, and that electrostatic effects are important as well.

Table 3. The effect of CO bond length on the upward offset of 3σ.

d_{C-O} [Å]	Total offset [eV]	Offset from bond length [eV]	Percentage [%]
1.120 (free)	0.0	0.00	0
1.149 (La on-top)	0.6	0.17	28
1.179 (Ni on-top)	2.0	0.70	35
1.205 (Ni–Ni bridge)	2.8	1.00	36

The overall electron transfer from the surface metal to the CO molecule or the dipole-like interfacial electronic distribution should contribute significantly to the upward shift of the electrostatic potential of electrons in the molecule.

On the other hand, changes in the other CO levels upon progressing from free CO to the adsorption systems seem to contain the effects of orbital mixing (hybridization) in addition to the effects of bond-length changes and electrostatic shifts. Table 4 lists the changes in the energy of each level relative to the 3σ level in each adsorption system. All the distances are similar to those of free CO in the La–CO on-top configuration, while the situations of the Ni–CO on-top and Ni–Ni–CO bridge adsorptions are quite different. The relative lowering is significant for the 5σ and 4σ levels of the latter two systems, which indicates that orbital mixing effects are significant for these levels in these two systems.

Regarding the La–CO on-top adsorption (Figure 4), the relative positions of the peaks are almost the same as those of the

Table 4. The offset of other peaks of CO relative to 3σ (as benchmark).

Site	$\Delta_{4\sigma-3\sigma}$ [eV]	$\Delta_{1\pi-3\sigma}$ [eV]	$\Delta_{5\sigma-3\sigma}$ [eV]
Free CO	15.24	17.47	20.26
La–CO on-top	15.01	17.55	19.24
Ni–CO on-top	13.97	17.01	16.62
Ni–Ni–CO bridge	12.98	16.47	15.92

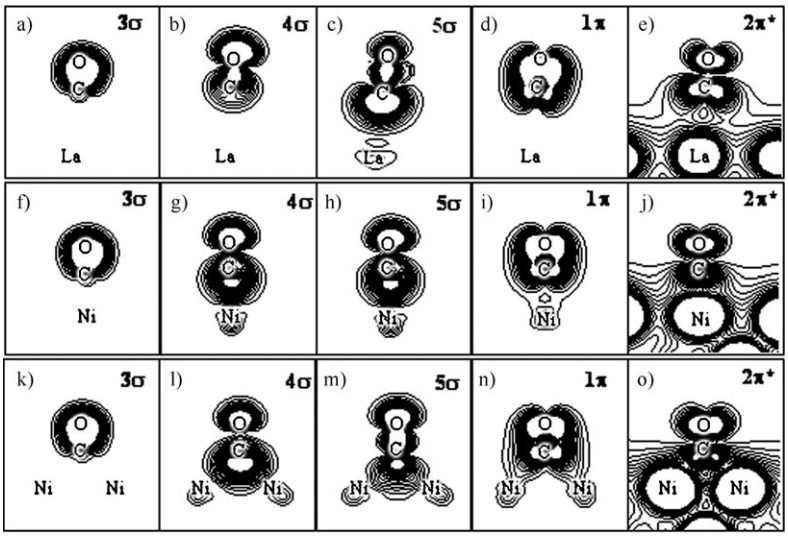

Figure 5. Charge density contour plots of some quantum states from the CO/La (a–e), CO/Ni (f–j), and CO/Ni–Ni (k–o) chemisorption systems.

corresponding peaks of free CO. With the exception of the orbital interactions of the $3dz^2$ orbital of the La atom with the 5σ and the partially occupied $2\pi^*$ orbitals of CO, there is no interaction among other orbitals, indicating a weak adsorption. This observation is in agreement with the poor electron transfer between CO and La (Figures 5a–e).

In the case of Ni–CO on-top adsorption (Figure 6), there is no interaction between the CO 3σ orbital and the Ni orbitals due to the huge energy differences between them, in addition

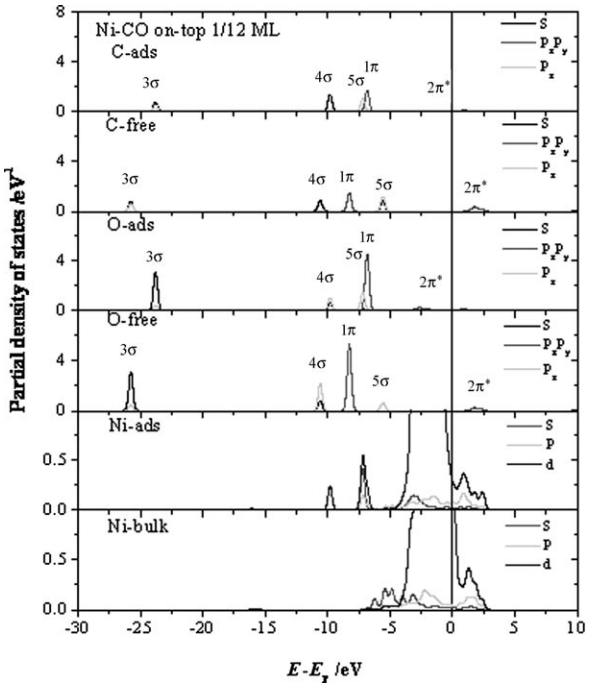

Figure 6. The PDOSs of CO on-top adsorption on a Ni atom of the $LaNi_5$ (001) surface ($\theta = 1/12$ ML). E_F is referenced as zero.

to the compactness of the 3σ CO wavefunction. On the other hand, the 4σ, 5σ and 1π orbitals of CO have much stronger interactions with those of the Ni atoms because of the substantial overlap from both the energy and the spatial viewpoints (Figure 5g–j). Due to its largest downward shift, the 5σ orbital of CO is mainly responsible for the interactions between CO and the substrate. It should be noted that the peak for the $2\pi^*$ orbitals, sitting above the Fermi energy level for free CO, become much broader and spread across the Fermi level, indicating that the $2\pi^*$ orbitals are partially occupied when adsorbed to the surface Ni atoms. This weakens the CO bond. The increase in CO bond length from 1.127 (before bonding) to 1.179 Å (after bonding) supports this finding. This should also be involved in the interfacial charge transfer (dipole-like distribution, Figure 7b). There is no orbital hybrid between σ (s–p_z) and π (p_x–p_y), indicating that the axis symmetry of CO is kept unchanged during CO adsorption.

Figure 8 shows the PDOS of the CO adsorption on the Ni–Ni bridge site. Except for the lowest 3σ orbital, the other orbitals obviously overlap with those of the Ni atoms. Compared to the Ni on-top adsorption, the shifts of the orbitals are much

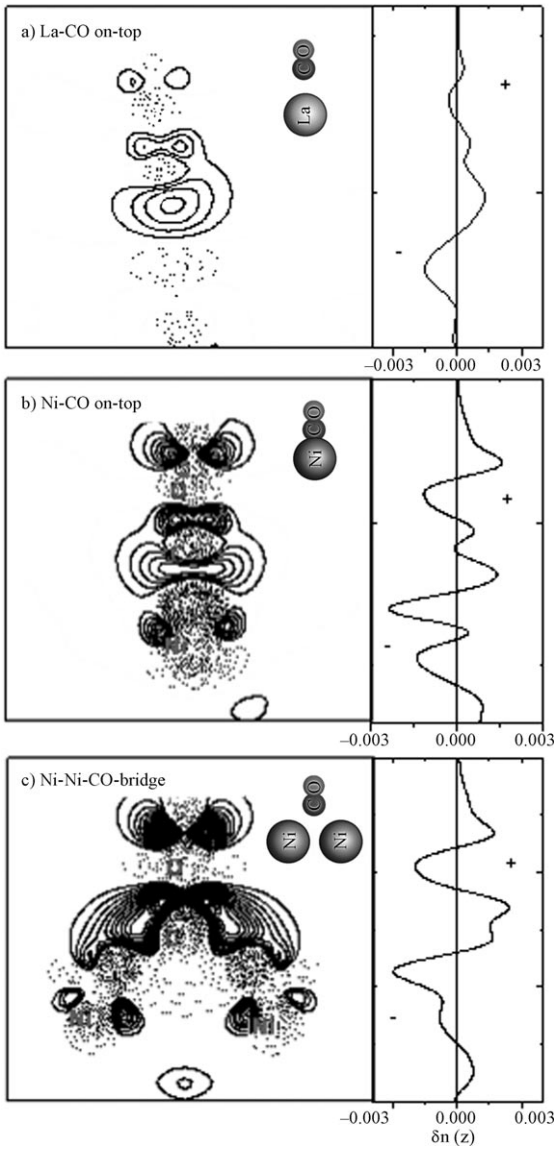

Figure 7. Charge redistribution and electron-transfer profiles on planes through a) C, O and La atoms for the La on-top adsorption configuration, b) C, O and Ni atoms for the Ni on-top adsorption configuration, and c) C, O and Ni atoms for the Ni–Ni bridge adsorption configuration. Contours of the different charge densities are plotted from −0.6 to 0.2 e Å^3 with a spacing of 0.013 e Å^3. Positive contours (——) denote charge accumulation and negative contours (•••••) indicate charge depletion.

larger, as listed in Tables 3 and 4, indicating a stronger interaction between CO and the surface Ni atoms. Moreover, the larger intensity of the $2\pi^*$ orbital (p_x–p_y) of O suggests that more electron density exists in the $2\pi^*$ anti-bonding orbital, which would further destabilize the C–O bond. This would result in a much longer C–O bond length (1.205 Å) and more significant charge transfer (or dipole-like distribution) at the interface (Figure 7c). Regarding the symmetry, except for the 5σ (s–p_z) and 1π (p_x–p_y) molecular orbitals, the axis symmetry is kept unchanged during CO adsorption. The bridge configuration is of high symmetry and CO is adsorbed with the carbon atom toward the surface.

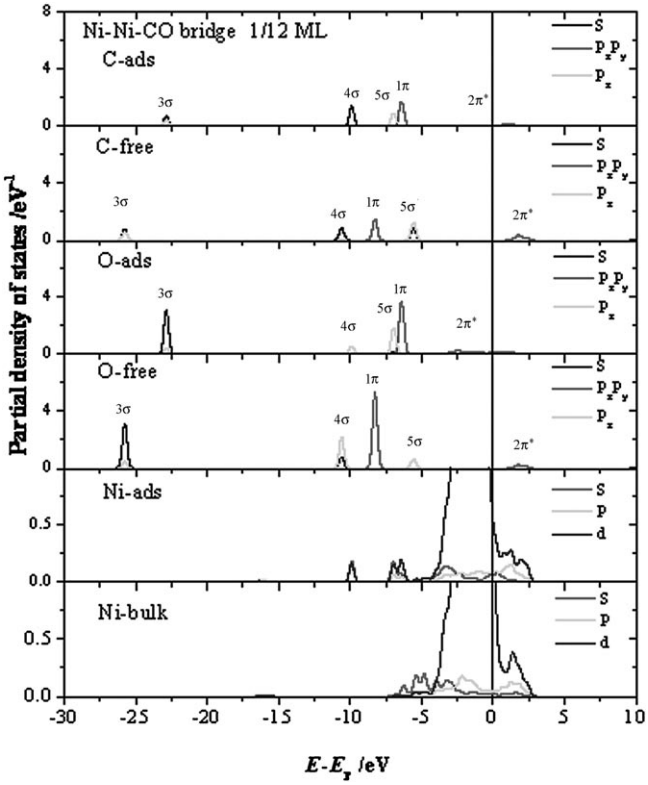

Figure 8. The PDOSs of CO bridge adsorption on two Ni atoms of the $LaNi_5$ (001) surface ($\theta = 1/12$ ML). E_F is referenced as zero.

To get a thorough insight into the chemical bonding, we examine the charge redistribution by subtracting the superposed charge density of the C and O atoms and the substrate with the same spatial coordinates as in the slab from the total charge density of the slab. Figures 7a–c shows the spatial and linear redistribution on the planes through the C and O atoms and the surface metal atoms for the La on-top, Ni on-top and Ni–Ni bridge CO adsorption, respectively. (——) denotes charge accumulation and (•••••) charge depletion. It can clearly be seen that the interfacial electron transfer is not so significant in La–CO on-top adsorption (Figure 7a), indicating that the interaction between CO and the La atoms is very weak. This is also confirmed by the small adsorption energy (0.462 eV). On the other hand, there are significant interfacial charge transfer or redistribution during the CO adsorptions on Ni on-top (Figure 7b) and Ni–Ni bridge (Figure 7c) sites, which should be the direct origin of the large rigid shifts of the levels as listed in Table 3 in addition to the bond-length effects.

3. Conclusions

We have investigated CO adsorption on the $LaNi_5$ (001) surface with DFT. At low coverages (1/12 ML), the most favored adsorption is at the Ni–Ni bridge site. With an increase in CO coverage, the decrease of the adsorption energy is much larger for the Ni–Ni–CO bridge adsorption than that for the Ni–CO on-top adsorption, and thus the latter only occurs in the relatively stable adsorption structure at high CO coverages (1/3, 2/3, and 1 ML). The results of the CO adsorption states on the $LaNi_5$ hydrogen storage alloys provide valuable information for understanding the deterioration mechanism during hydrogen storage process with CO-contaminated hydrogen. Further DFT calculations on co-adsorption of CO/H_2 mixture on the $LaNi_5$ surface are underway.

Acknowledgements

The present work is financially supported by AIST and NEDO.

Keywords: adsorption · alloys · density functional calculations · hydrogen storage · surface chemistry

[1] A. C. Dillon, K. M. Jones, T. A. Bekkedahl, C. H. Kiang, D. S. Bethune, M. J. Heben, *Nature* **1997**, *386*, 377.
[2] C. Liu, Y. Y. Fan, M. Liu, H. T. Cong, H. M. Cheng, M. S. Dresselhaus, *Science* **1999**, *286*, 1127.
[3] P. Chen, Z. T. Xiong, J. Z. Luo, J. Y. Lin, K. L. Tan, *Nature* **2002**, *420*, 302.
[4] L. Schlapbach, A. Zuttel, *Nature* **2001**, *414*, 353.
[5] J. H. N. van Vucht, F. A. Kuijpers, H. C. A. M. Bruning, *Philips Res. Rep.* **1970**, *25*, 133.
[6] W. K. Hu, *J. Alloys Compd.* **1999**, *289*, 299.
[7] A. J. Du, S. C. Smith, X. D. Yao, G. Q. Lu, *J. Phys. Chem. B* **2005**, *109*, 18037.
[8] J. J. Liang, W. C. P. Kung, *J. Phys. Chem. B* **2005**, *109*, 17837.
[9] S. Han, X. Zhang, S. Shi, H. Tanaka, N. Kuriyama, N. Taoka, K. Aihara, Q. Xu, *J. Alloys Compd.* **2007**, *446–447*, 208.
[10] N. M. Markovic, P. N. Ross, *Electrochim. Acta* **2000**, *45*, 4101.
[11] P. D. Goodell, G. D. Sandrock, E. L. Huston, *J. Less-Common Met.* **1980**, *73*, 135.
[12] H. Tanaka, N. Kuriyama, S. Ichikawa, H. Senoh, N. Naka, K. Aihara, H. Itoh, M. Tsukahara, *In Pricm 5: The Fifth Pacific Rim International Conference on Advanced Materials and Processing, Pts 1–5*; Trans. Tech Publications Ltd: Zurich–Uetikon, **2005**, Vol. 475–479, p 2481.
[13] H. Tanaka, H. Senoh, N. Kuriyama, K. Aihara, N. Terashita, T. Nakahata, *Mater. Sci. Eng. B* **2004**, *108*, 81.
[14] T. Matsushima, *Surf. Sci. Rep.* **2003**, *52*, 1.
[15] Q. Ge, R. Kose, D. A. King, C. G. Bruce, K. Helmut, in *Adv. Catal. Vol. 45*, (Eds: C. G. Bruce, K. Helmut), **2000**, 207, Academic Press, San Diego.
[16] W. A. Brown, R. Kose, D. A. King, *Chem. Rev.* **1998**, *98*, 797.
[17] M. Lynch, P. Hu, *Surf. Sci.* **2000**, *458*, 1.
[18] A. Eichler, *Surf. Sci.* **2003**, *526*, 332.
[19] S. Corré, D. Fruchart, G. Y. Adachi, *J. Alloys Compd.* **1998**, *264*, 164.
[20] S. Gonzalez, C. Sousa, F. Illas, *Surf. Sci.* **2003**, *531*, 39.
[21] Y. G. Shen, D. J. O'Connor, R. J. MacDonald, *Aust. J. Phys.* **1996**, *49*, 689.
[22] G. Kresse, J. Furthmuller, *Phys. Rev. B* **1996**, *54*, 11169.
[23] G. Kresse, J. Hafner, *Phys. Rev. B* **1993**, *47*, 558.
[24] G. Kresse, J. Hafner, *Phys. Rev. B* **1994**, *49*, 14251.
[25] P. E. Blöchl, *Phys. Rev. B* **1994**, *50*, 17953.
[26] G. Kresse, D. Joubert, *Phys. Rev. B* **1999**, *59*, 1758.
[27] J. P. Perdew, Y. Wang, *Phys. Rev. B* **1992**, *45*, 13244.
[28] H. J. Monkhorst, J. D. Pack, *Phys. Rev. B* **1976**, *13*, 5188.
[29] C. L. Fu, K. M. Ho, *Phys. Rev. B* **1983**, *28*, 5480.
[30] J. Neugebauer, M. Scheffler, *Phys. Rev. B* **1992**, *46*, 16067.
[31] D. R. Lide, *CRC Handbook of Chemistry and Physics*, 79th ed., CRC Press, Boca Raton, **1998**).
[32] J. T. Hoeft, M. Polcik, D. I. Sayago, M. Kittel, R. Terborg, R. L. Toomes, J. Robinson, D. P. Woodruff, M. Pascal, G. Nisbet, C. L. A. Lamont, *Surf. Sci.* **2003**, *540*, 441.
[33] E. W. Plummer, W. R. Salaneck, J. S. Miller, *Phys. Rev. B* **1978**, *18*, 1673.

Received: February 6, 2008
Revised: May 12, 2008
Published online on June 20, 2008

